J Therm Anal Calorim (2012) 108:887–894
DOI 10.1007/s10973-012-2355-x

Synthesis growth and characterization of L-valine nickel (II) chloride

A novel semiorganic nonlinear optical crystal

M. K. Sangeetha · M. Mariappan · G. Madhurambal · S. C. Mojumdar

CTAS2011 Conference Special Chapter

Abstract A new semi organic nonlinear optical crystal, L-valine nickel chloride has been synthesized and good optical quality single crystals were grown by slow evaporation technique. The growth conditions of the crystals are studied and the grown crystals are confirmed by powder X-ray diffraction studies. The grown crystal was characterized by using powdered XRD, FT-IR, UV–Vis–NIR, EDAX, and TG–DTA. The crystalline nature and its various planes of reflections were observed by the powder XRD. The presence of various functional groups was confirmed by FT-IR spectroscopic technique. The UV–Vis–NIR spectrum indicates that the crystal has very good absorption in the entire visible and near IR region spectrum suggesting the suitability of the material for NLO applications. The decomposition temperatures and mass loss have been estimated from the thermogravimetric analysis.

M. K. Sangeetha
AVC College of Engineering, Mannampandal, Mayiladuthurai, India

M. Mariappan
H. H. The Rajah's College, Pudukkottai, Pudukottai District, India

G. Madhurambal
A. D. M. College for Women, Nagapattinam 611001, Tamil Nadu, India

S. C. Mojumdar (✉)
Department of Chemistry, University of Guelph, Guelph, ON, Canada
e-mail: scmojumdar@yahoo.com

S. C. Mojumdar
Department of Chemical Technologies and Environment, Faculty of Industrial Technologies, Trenčín University of A. Dubček, SK-02032 Púchov, Slovakia

Keywords L-Valine nickel chloride · Infrared spectrum · UV–Vis–NIR spectrum · Thermal analysis

Introduction

In the modern world, the development of science in many areas has been achieved through the growth of single crystals. Nonlinear optical (NLO) materials are expected to play a major role in the technology of photonics including optical information processing. Many research efforts are undertaken to synthesize and characterize new molecules for second-order NLO applications such as high-speed information processing, optical communications, and optical data storage [1–12]. These applications depend on the various properties of the materials, such as transparency, birefringence, refractive index and dielectric constant, thermal, photochemical, and chemical stability. Among NLO materials, organic NLO materials are generally believed to be more versatile than their inorganic counterparts due to their more favorable nonlinear response. In the organic class, R-amino acids exhibit some specific features such as molecular chirality, weak Vander Waals and hydrogen bonds, the absence of strongly conjugated bonds, wide transparency ranges in the visible and UV spectral regions, and zwitterionic nature of the molecule which favors crystal hardness. Other advantages of organic compounds apart from the above include amenability for synthesis, multifunctional substitutions, higher resistance to optical damage and maneuverability for device applications etc. [13–18]. The importance is due to the fact that amino acids contain chiral carbon atom and crystallize in the noncentrosymmetric space groups, therefore, they are potential candidates for optical second harmonic generation. Thermal, XRD, microscopic, and spectral analyses are very useful methods

for materials characterization. Therefore, many authors have used these techniques for various materials characterization [19–39]. The present investigation deals with the growth of L-valine nickel chloride (LVNiC) an analog of L-valine single crystal by slow solvent evaporation technique. The grown crystal was subjected to powder XRD, FT-IR, UV–Vis–NIR, SEM, EDAX, and TG-DSC.

Experimental methods

Synthesis and growth technique

The starting material was synthesized by taking L-valine (AR grade) and nickel(II)chloride hexahydrate (AR grade) in a 1:1 stoichiometric ratio. The required amount of starting materials for the synthesis of LVNiC crystal was calculated according to the following reaction:

$$C_5H_{11}NO_2 + NiCl_2 \cdot 6H_2O \rightarrow Ni\ [C_5H_{11}NO_2]\ Cl_2$$

The calculated amount of nickel chloride hexahydrate was first dissolved in acetic acid. L-Valine was then added to the solution. The solution was stirred for 15 min continuously and heated for 15 min till complete dissolution of the starting materials. The prepared solution was filtered and allowed to dry at room temperature. The crystals were obtained by slow evaporation technique. The purity of the synthesized crystal was further improved by successive recrystallization process; thereby good optical qualities of single colorless crystals were obtained in 60 days.

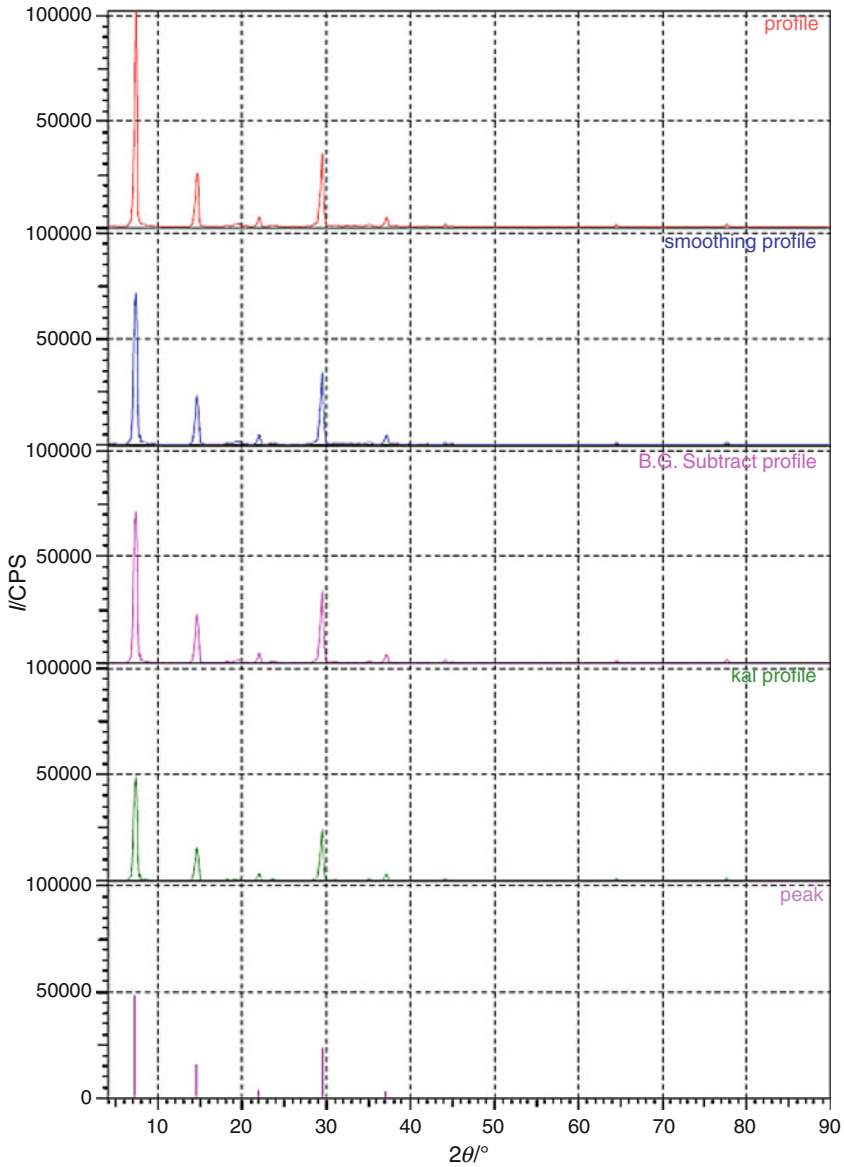

Fig. 1 Powder XRD analysis of L-valine

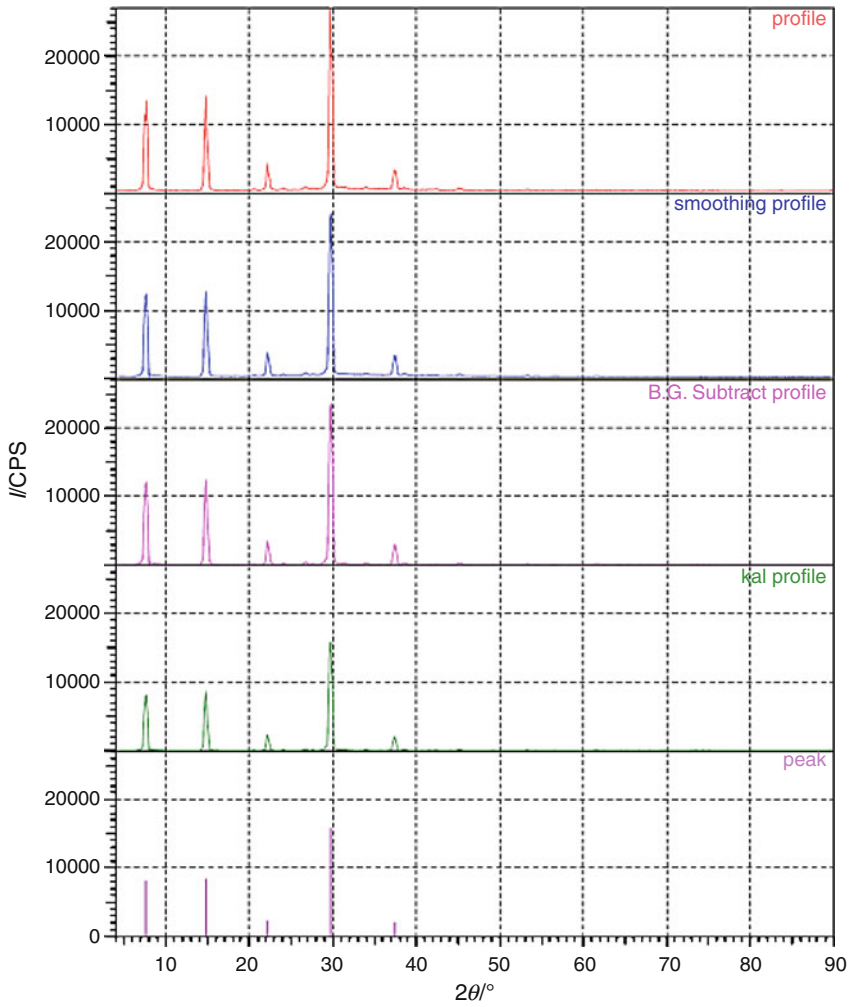

Fig. 2 Powder XRD analysis of L-valine nickel chloride

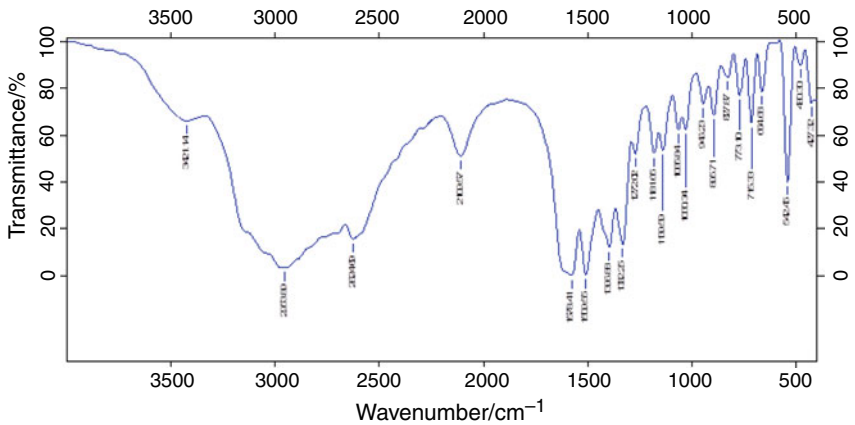

Fig. 3 FTIR spectrum of L-valine

Measurements

Powder X-ray diffraction studies of L-valine and LVNiC crystal were carried out on a Siemens D500 X-ray diffractometer with Cu Kα ($\lambda = 1.5418$ Å) radiation. The samples were scanned for 2θ values from 10 to 50° at a rate of 2° min^{-1}.

The infrared spectra of L-valine and LVNiC were obtained from potassium bromide pellets technique using MAKE–BRUKER Optic GmbH MODEL No-TENSOR 27 SOFTWARE-OPUS version 6.5 Spectrophotometer in the range of 4,000–400 cm^{-1}.

Differential scanning calorimetric analysis (DSC) and thermogravimetric analysis (TG) were carried out

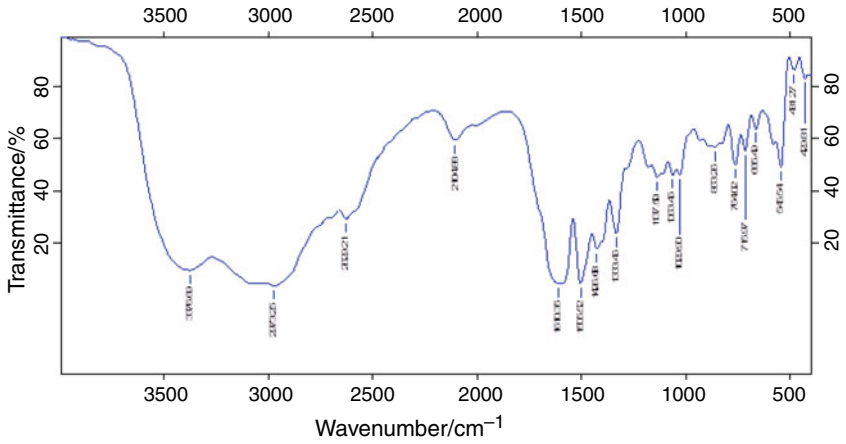

Fig. 4 FTIR spectrum of L-valine nickel chloride

Table 1 Comparison of FTIR spectra of L-valine and LVNiC

Wave number/cm^{-1}		Assignments
L-Valine	LVNiC	
2,953	2,973	CH_2 symmetric stretching
2,624	2,629	N–H–O combination
1,578	1,610	COO^- asymmetric stretching
1,509	1,505	NH_3 deformation
1,396	1,426	COO^- asymmetric stretching
1,332	1,333	C–O stretching
1,272	1,137	C–C stretching
1,181	1,063	C–C stretching
1,139	1,029	C–C–N stretching
1,064	863	NH_3 rocking
1,030	764	C–H deformation
946	715	C–C–O deformation
773	481	C–C deformation

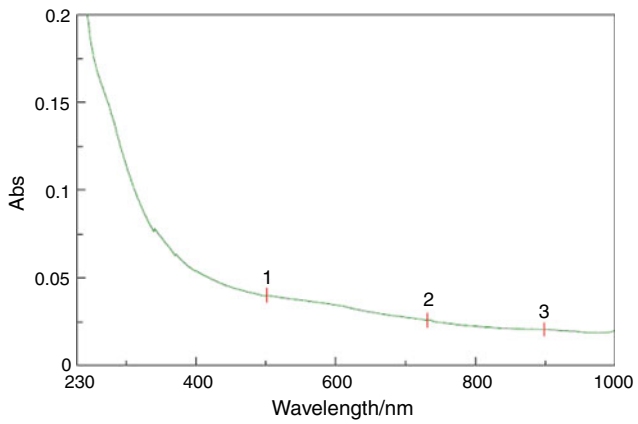

Fig. 5 UV–VIS–NIR spectrum of L-valine

simultaneously on a TA Instruments SDT Q600 V20.9 Build 20. The sample was heated at a rate of 10 °C min^{-1} in protected nitrogen gas flow and 10.6740 mg of the sample was used to carry out the experiment.

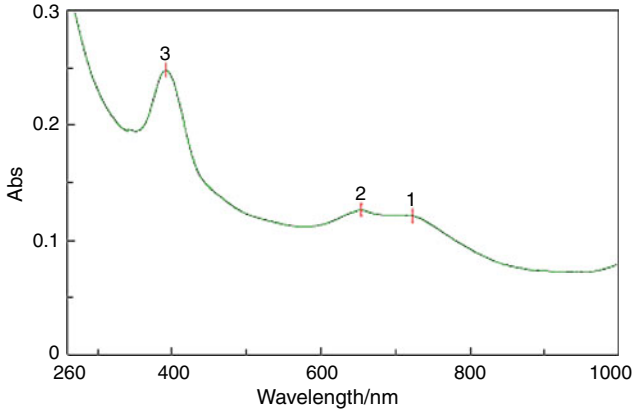

Fig. 6 UV–Vis–NIR spectrum of L-valine nickel chloride

The UV–Vis–NIR spectra were recorded on a Jasco V-630 spectrophotometer in the range of 200–1,100 nm with scanning speed of 400 nm min^{-1}.

SEM analysis was carried out on a JSM 6360 JEOL/EO. The surface of the crystal was coated with a thin of carbon to make the sample conducting.

Results and discussion

Powder XRD studies

The structural property of the single crystals of LVNiC was studied by X-ray powder diffraction technique. Powder XRD pattern of L-valine was given in Fig. 1. Figure 2 shows the powder XRD pattern of the pure LVNiC crystal. The diffraction patterns of LVNiC crystal have been indexed by least square fit method. The lattice parameter values of crystal were calculated and are matched with the reported literature. The lattice parameters are $a = 7.5940$ Å, b = 14.7958 Å, c = 29.7454 Å, volume 3342.1724.

FT-IR spectral studies

The infrared spectra of L-valine and LVNiC are shown in Figs. 3 and 4, respectively. The IR spectra of LVNiC mainly arise due to internal vibration of functional groups NH^{3+}, CH, CH_3, and COOH. The absorptions of LVNiC have been compared with those of the parent compound (L-valine) in Table 1. The broad peak at 2,973 cm^{-1} is due to the methylene symmetric stretching. The N–H–O valance stretching combination observed at 2,629 cm^{-1}. The sharp peaks at 1,505 and 1,333 cm^{-1} are due to COO^- asymmetric and symmetric stretching mode of vibrations. The deformation bands observed at 1,505 cm^{-1} is due to the protonated amino group NH^{3+}. The C–C stretching modes are observed at 1,137 and 1,063 cm^{-1}. The sharp peak at 1,029 cm^{-1} is due to C–C–N stretching mode. The C–H out-of plane bending and C–CO deformation are observed at 764 and 715 cm^{-1}, respectively.

UV–Vis–NIR spectral analysis

To find the optical absorption range of LVNiCL crystals, the UV–Vis–NIR spectra (Figs. 5, 6) were used. When the absorption is monitored from longer to shorter wavelengths, optical absorption with lower cut-off wavelength below 392 nm for LVNiCL, which is sufficient for SHG laser radiation of 1,064 nm and the transmittance of the crystal, is about 90% in the entire visible and infrared region.

TG-DSC studies

Figure 7 shows the TG and DSC curves of L-valine and Fig. 8 shows the TG and DSC curves of LVNiC. From DSC curve (Fig. 7), it is observed that the material undergoes an irreversible exothermic transition at about 220 °C where the decomposition starts, which indicate the

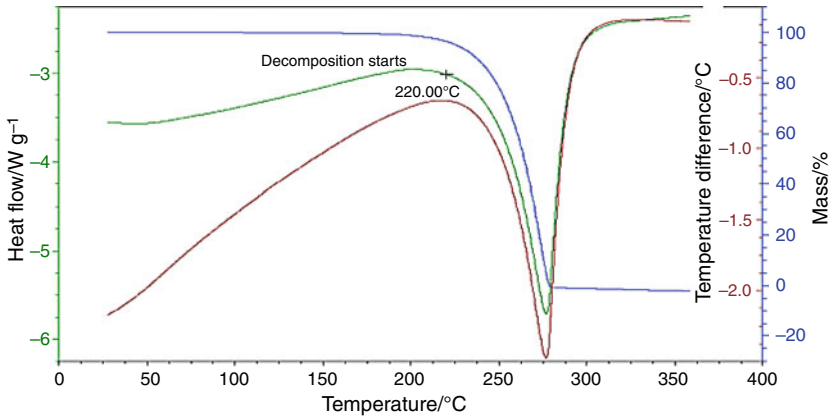

Fig. 7 TG-DSC curves of L-valine

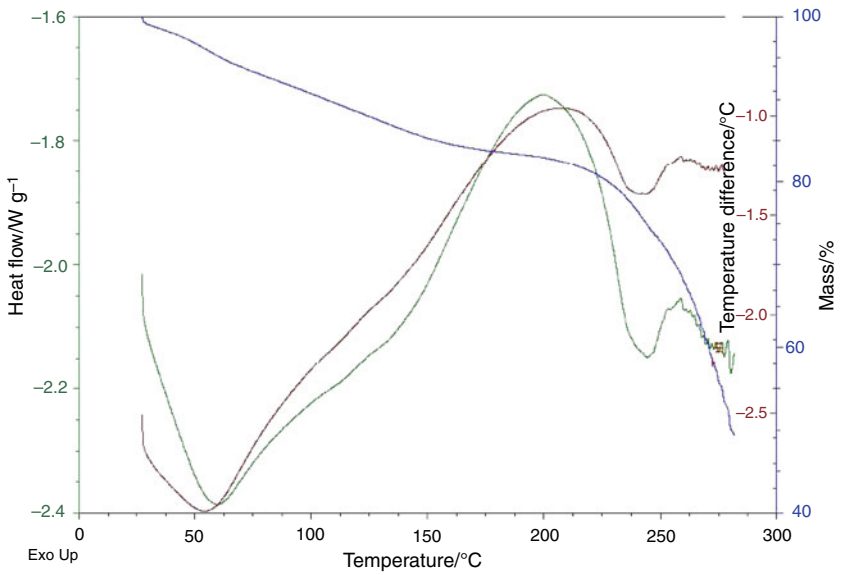

Fig. 8 TG-DSC curves of L-valine nickel chloride

material stable up to 220 °C. L-Valine is fully decomposed at 300 °C. The sharpness of the exothermic peak shows good degree of crystallinity of the grown crystals. It can be seen also on the TG curve that the mass loss starts at 220 °C and ends at about 300 °C. This mass loss is due to the liberation of volatile substances. The peak at 280 °C indicates a phase change from liquid to vapor state as evidence from the loss of mass on the TG curve. The TG-DSC analyses do not show any kind of phase transition of LVNiC crystal.

Crystal surface analysis by SEM

SEM analysis was used to study the morphology of LVNiC and is given in Fig. 9. From the Fig. 9, the following observations are evident

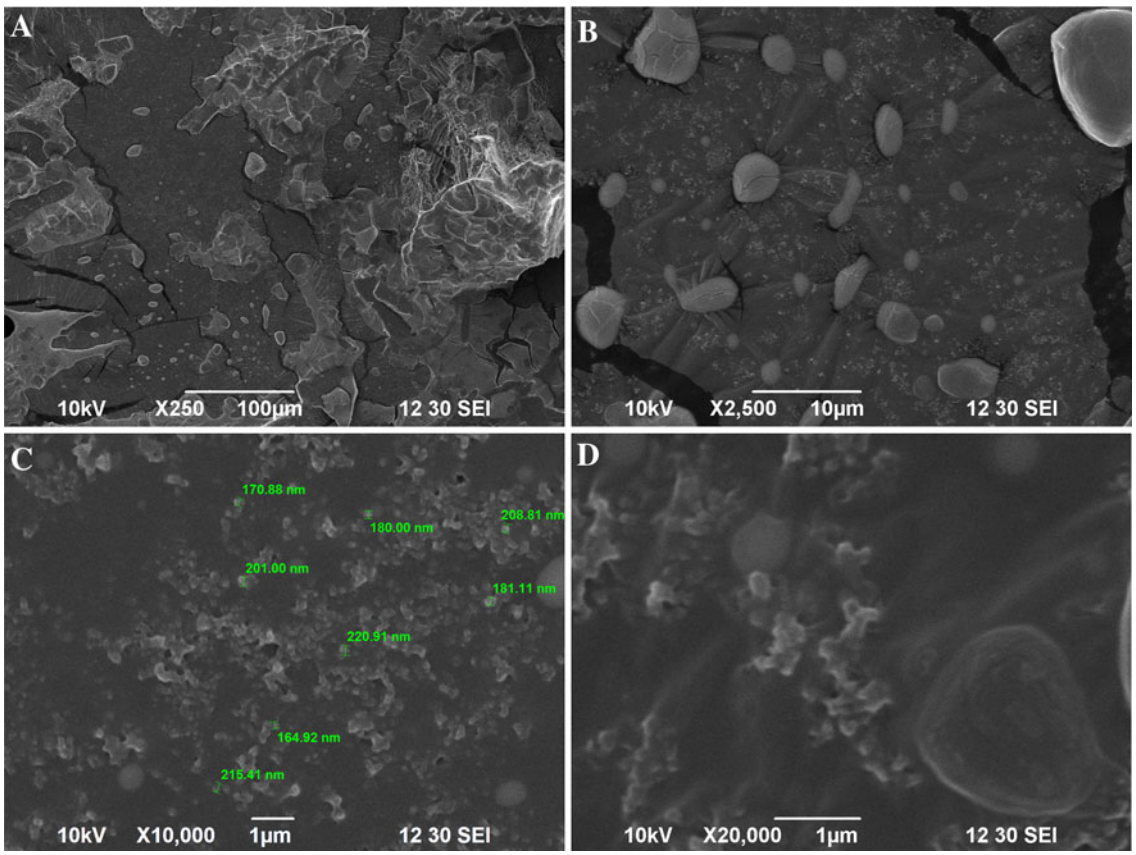

Fig. 9 **a** SEM image of L-valine nickel chloride. **b** SEM image of L-valine nickel chloride. **c** SEM image of L-valine nickel chloride. **d** SEM image of L-valine nickel chloride

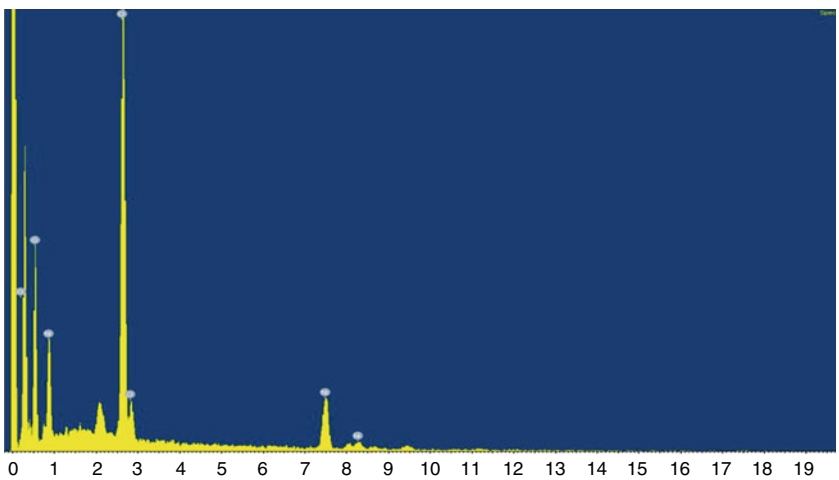

Fig. 10 Energy dispersive X-ray analysis of L-valine nickel chloride

Table 2 EDX analysis of LVNiC

Element	Spectral Type	Element/%	Atomic/%
O	ED	48.41	70.87
Cl	ED	32.66	21.57
Ni	ED	18.93	7.55
Total		100.00	100.00

(1) At a magnifications of 250 and at a scale of 100 μm we observe the crystals have smoothed surfaces.
(2) At a magnifications of 2,500 and 10 μm scale we can observe that the crystals have an average thickness of 2.56 μm.
(3) At a magnifications of 10,000 and at a scale of 1 μm we can observe that crystals have an average thickness of 181.00 nm.

Energy dispersive X-ray analysis

In order to confirm the presence of the elements of LVNiC crystals, the sample of grown crystals were subjected to energy dispersive X-ray analysis on a JEOL-6360 scanning electron micro-scope. Figure 10 shows the EDX result of LVNiC crystals. Elements are identified and presented as atomic% (Table 2).

Conclusions

The seed crystals of L-valine nickel chloride crystals (LVNiCL) are grown from the solution prepared from the raw materials L-valine and nickel chloride. These crystals are characterized and the following results are obtained.

(1) The grown crystals are characterized by using powder XRD diffraction. From this we confirm the structure of the crystal to be triclinic and the cell parameters are as follows.

Crystal system
Space group

a = 7.5940 (3) Å
b = 14.7958(2) Å
c = 29.7454 (1) Å
Volume = 3342.1724

(2) From the FTIR spectrum we confirm the structure of the LVNiCL to have both the L-valine and nickel chloride molecules. These arrangements are in alternate layers in the crystal. This is evident from the non damage of L-valine structure.
(3) From the UV–Visible spectrum we find the crystal is transparent in the range of 200–1,100 nm.
(4) The sharpness of the exothermic peak shows good degree of crystallinity of the grown crystals and indicates its suitability for application in lasers field.
(5) From the SEM analysis we conclude that the crystal formation size in micro range is 293.17. Further in the micro level the crystal surface is very smooth which shows that it can add more molecules to grow into a large crystal.
(6) EDAX confirm the presence of the elements of LVNiCL.

References

1. Krishnan H, Justin C, Jerome S. Growth and characterization of novel ferroelectric urea-succinic acid single crystals. J Cryst Growth. 2008;310:3313–7.
2. Gupte SS, Desai CF. Vickers hardness anisotropy and slip system in zinc(tris)thioureasulphate crystals. Cryst Res Technol. 1999; 34:1329–32.
3. Verma S, Singh MK, Wadhavan VK, Suresh CH. Growth morphology of zinctris(thiourea)sulphate crystals. J Phys. 2000;54: 879–84.
4. Boomadevi S, Dhanasekaran R, Ramasamy P. Investigation on nucleation kinetics of urea crystals from methanol. Cryst Res Technol. 2002;37:159–68.
5. Sangwal K, Mielniczek-Brzoska E. Effect of impurities on metastable zone width for the growth of ammonium oxalate monohydrate crystals from aqueous solutions. J Cryst Growth. 2004;267:662–75.
6. Li G, Xue L, Su G, Li Z, Zhuang X, He Y. Rapid growth of KDP crystal from aqueous solutions with additives and its optical studies. Cryst Res Technol. 2005;40:867–70.
7. Gunasekaran S, Ponnusamy S. Growth and characterization of cadmium magnesium tetra thiocyanate crystals. Cryst Res Technol. 2006;41:130–7.
8. Udayalakshmi K, Ramamurthi K. Optical, mechanical and thermal properties of p-bromoacetanilide. Cryst Res Technol. 2006; 41:795–9.
9. Kumar K, Ramamurthy K. A novel growth method for zinc thiourea sulphate single crystals. Cryst Res Technol. 2006;41: 217–20.
10. Rajasekaran R, Rajendran KV. Investigation on nucleation of cadmium thiourea chloride single crystals. Mater Chem Phys. 2003;82:273–80.
11. Angelimary PA, Dhanuskodi S. Growth and characterization of a new nonlinear optic Bisthiourea zinc chloride. Cryst Res Technol. 2001;36:1231–7.
12. Hameed SH, Ravi G, Dhanasekaran R, Ramasamy P. Growth and characterization of KDP and KAP. J Cryst Growth. 2000;212: 227–34.
13. Madhurambal G, Mojumdar SC, Hariharan S, Ramasamy P. TG, DTC, FT-IR and Raman spectral analysis of Zn_a/Mg_b ammonium sulfate mixed crystals. J Therm Anal Cal. 2004;78:125–33.
14. Kuznetsov VA, Okhrimenko TM, Rak M. Growth promoting effect of organic impurities on growth kinetics of KAP and KDP crystals. J Cryst Growth. 1998;193:164–73.
15. Zaitseva NP, Rashkovich LN, Bogatyreva SV. Stability of KH2PO4 and K(H, D)2PO4 solutions at fast crystal growth rates. J Cryst Growth. 1995;148:276–82.

16. Nyvlt J, Rychly R, Gottfried J, Wurzelova J. Metastable zone-width of some aqueous solutions. J Cryst Growth. 1970;6:151–62.
17. Rak M, Eremin NN, Eremina TA, Kuznetsov VA, Okhrimenko TM, Furmanova NG, Efremova EP. On the mechanism of impurity influence on growth kinetics and surface morphology of KDP crystals-I: defect centers formed by bivalent and trivalent impurity ions incorporated in KDP structure-theoretical study. J Cryst Growth. 2005;273:577–85.
18. Ushasree PM, Jayavel R, Ramasamy P. Growth and characterization of phosphate mixed ZTS single crystals. Mater Sci Eng B. 1999;65:153–8.
19. Mojumdar SC, Raki L. Preparation, thermal, spectral and microscopic studies of calcium silicate hydrate-poly(acrylic acid) nanocomposite materials. J Therm Anal Calorim. 2006;85:99–105.
20. Sawant SY, Verenkar VMS, Mojumdar SC. Preparation, thermal, XRD, chemical and FT-IR spectral analysis of $NiMn_2O_4$ nanoparticles and respective precursor. J Therm Anal Calorim. 2007;90:669–72.
21. Porob RA, Khan SZ, Mojumdar SC, Verenkar VMS. Synthesis, TG, SDC and infrared spectral study of $NiMn_2(C_4H_4O_4)_3 \cdot 6N_2H_4$—a precursor for $NiMn_2O_4$ nanoparticles. J Therm Anal Calorim. 2006;86:605–8.
22. Mojumdar SC, Varshney KG, Agrawal A. Hybrid fibrous ion exchange materials: past, present and future. Res J Chem Environ. 2006;10:89–103.
23. Doval M, Palou M, Mojumdar SC. Hydration behaviour of C_2S and C_2AS nanomaterials, synthesized by sol-gel method. J Therm Anal Calorim. 2006;86:595–9.
24. Mojumdar SC, Moresoli C, Simon LC, Legge RL. Edible wheat gluten (WG) protein films: preparation, thermal, mechanical and spectral properties. J Therm Anal Calorim. 2011;104:929–36.
25. Varshney G, Agrawal A, Mojumdar SC. Pyridine based cerium(IV) phosphate hybrid fibrous ion exchanger: synthesis, characterization and thermal behaviour. J Therm Anal Calorim. 2007;90:731–4.
26. Mojumdar SC, Melnik M, Jona E. Thermal and spectral properties of Mg(II) and Cu(II) complexes with heterocyclic N-donor ligands. J Anal Appl Pyrolysis. 2000;53:149–60.
27. Borah B, Wood JL. Complex hydrogen bonded cations. The benzimidazole benzimidazolium cation. Canad J Chem. 1976;50:2470–81.
28. Mojumdar SC, Sain M, Prasad RC, Sun L, Venart JES. Selected thermoanalytical methods and their applications from medicine to construction. J Therm Anal Calorim. 2007;60:653–62.
29. Meenakshisundarm SP, Parthiban S, Madhurambal G, Mojumdar SC. Effect of chelating agent (1,10-phenanthroline) on potassium hydrogen phthalate crystals. J Therm Anal Calorim. 2008;94:21–5.
30. Rejitha KS, Mathew S. Investigations on the thermal behavior of hexaamminenickel(II) sulphate using TG-MS and TR-XRD. Glob J Anal Chem. 2010;1(1):100–8.
31. Pajtášová M, Ondrušová D, Jóna E, Mojumdar SC, Ľalíková S, Bazyláková T, Gregor M. Spectral and thermal characteristics of copper(II) carboxylates with fatty acid chains and their benzothiazole adducts. J Therm Anal Calorim. 2010;100:769–77.
32. Madhurambal G, Ramasamy P, Anbusrinivasan P, Vasudevan G, Kavitha S, Mojumdar SC. Growth and characterization studies of 2-bromo-4′-chloro-acetophenone (BCAP) crystals. J Therm Anal Calorim. 2008;94:59–62.
33. Gonsalves LR, Mojumdar SC, Verenkar VMS. Synthesis and characterisation of $Co_{0.8}Zn_{0.2}Fe_2O_4$ nanoparticles. J Therm Anal Calorim. 2011;104:869–73.
34. Raileanu M, Todan L, Crisan M, Braileanu A, Rusu A, Bradu C, Carpov A, Zaharescu M. Sol-gel materials with pesticide delivery properties. J Environ Prot. 2010;1:302–13.
35. Varshney KG, Agrawal A, Mojumdar SC. Pectin based cerium(IV) and thorium(IV) phosphates as novel hybrid fibrous ion exchangers synthesis, characterization and thermal behaviour. J Therm Anal Calorim. 2005;81:183–9.
36. Mojumdar SC, Šimon P, Krutošíková A. [1]Benzofuro[3,2-c]pyridine: synthesis and coordination reactions. J Therm Anal Calorim. 2009;96:103–9.
37. Moricová K, Jóna E, Plško A, Mojumdar SC. Thermal stability of Li_2O–SiO_2–TiO_2 gels evaluated by the induction period of crystallization. J Therm Anal Calorim. 2010;100:817–20.
38. Mojumdar SC, Miklovic J, Krutosikova A, Valigura D, Stewart JM. Furopyridines and furopyridine-Ni(II) complexes—synthesis, thermal and spectral characterization. J Therm Anal Calorim. 2005;81:211–5.
39. Vasudevan G, AnbuSrinivasan P, Madhurambal G, Mojumdar SC. Thermal analysis, effect of dopants, spectral characterisation and growth aspects of KAP crystals. J Therm Anal Calorim. 2009;96:99–102.